Ion-Selective Optode Nanospheres as Heterogeneous Indicator Reagents in Complexometric Titrations

ARTICLE *in* ANALYTICAL CHEMISTRY · JANUARY 2015

Impact Factor: 5.64 · DOI: 10.1021/ac504213q · Source: PubMed

3 AUTHORS:

Jingying Zhai
University of Geneva
13 PUBLICATIONS **57** CITATIONS
SEE PROFILE

Xiaojiang Xie
University of Geneva
32 PUBLICATIONS **277** CITATIONS
SEE PROFILE

Eric Bakker
University of Geneva
291 PUBLICATIONS **13,796** CITATIONS
SEE PROFILE

analytical chemistry

Article

pubs.acs.org/ac

Ion-Selective Optode Nanospheres as Heterogeneous Indicator Reagents in Complexometric Titrations

Jingying Zhai, Xiaojiang Xie, and Eric Bakker*

Department of Inorganic and Analytical Chemistry, University of Geneva, Quai Ernest-Ansermet 30, CH-1211 Geneva, Switzerland

Supporting Information

ABSTRACT: Traditionally, optical titrations of inorganic ions are based on a rapid and visible color change at the end point with water-soluble organic dyes as indicators. Adequate selectivity is required for both the indicator and the complexing agent, which is often limited. We present here alternative, heterogeneous ionophore-based ion-selective nanospheres as indicators and chelators for optical titrations. The indicating nanospheres rely on a weaker extraction of the analyte of interest by ion-exchange, owing to the additional incorporation of a lipophilic pH indicator in the nanosphere core. Ca^{2+} titration was demonstrated as a proof-of-concept. Both the chelating and the indicating nanospheres showed good selectivity and a wide working pH range.

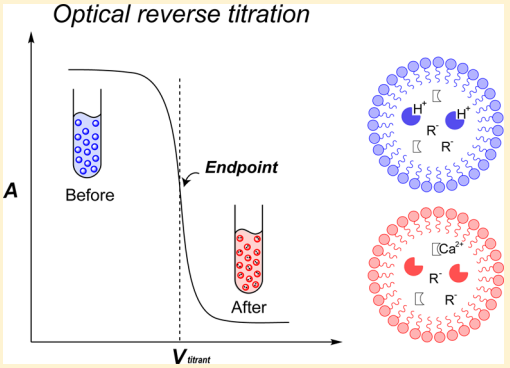

Complexometric titration is a mature analytical technique that is being taught all over the world in analytical science.[1,2] Titrations are routinely used to determine ion concentration, speciation as well as complexation reactions in various fields such as environmental, clinical, and bioanalytical chemistry.[3−6]

Water-soluble organic compounds have been applied as chelators for complexometric titrations for over 60 years.[2,3,7] However, their pH-dependent complexing ability and rather rigid selectivity remain an issue.[1,2,8] We have recently introduced colloidal titration reagents that may dramatically increase the available chemical toolbox of possible titration reagents, alleviate the need for pH control, and eliminate the requirement of a defined and singular reaction stoichiometry.[9]

The titration end point may typically be detected with optical indicators or electrochemical sensors.[6,10] An optical indicator, also a chelating agent, is easy to handle compared with electrochemical sensors owing to the convenient visual color change at the end point. Organic dyes that directly bind to the analyte ion are typically used as optical indicators in chelometry. Current examples include phenolphthalein,[11] methyl red,[12] fast sulphon black,[13] Eriochrome Black T,[14] and murexide.[15]

As an optical indicator, the metal-indicator complex must be at least 10 to 100 times less stable than the metal-chelator complex so that the chelator can effectively displace the ion from the indicator complex. An indicator should have good selectivity, rapid and visible change in color, and be water-soluble and stable. Not all available optical indicators can fulfill these requirements.[1]

Numerous indicators are weak acids, such as Eriochrome Black T, a classical indicator for determination of water hardness.[14] As a weak acid, its color will also depend on the sample pH. In addition, the stability of metal−indicator complex and metal−chelator complex are pH-dependent as well, and these types of experiments require careful pH control.[2]

Moreover, some optical indicators do not exhibit good selectivity. For example, murexide is used as an indicator for several metal ions including Ca^{2+}, Cu^{2+}, Ni^{2+}, and Co^{2+}.[15,16] A bias in the observed end point may arise in cases where these ions coexist in the sample.

Ionophore-based optical ion sensors (optodes) have been known for many years.[17−19] However, their application as end point indicator for titration applications has not yet been put forward. The sensor must exhibit sufficient sensitivity to act as end point indicator. It is also known that the optode response is pH-dependent, and therefore, it requires pH control. Recently, an exhaustive sensing mode for ion-selective optodes has been proposed.[20,21] The exhaustive nanosensors exhibited low detection limit, short response time, and may largely overcome any pH cross-response.

Here, we report for the first time that titrimetric analysis can be performed with ion-selective nanospheres acting both as chelators and indicators, thereby moving the conventional homogeneous titration in aqueous phase to a heterogeneous emulsion-based organic−aqueous environment. pH-independent titrations for Ca^{2+} were achieved by using exhaustive calcium-selective optical nanospheres as end point indicator, and calcium-selective nanospheres containing no chromoionophore were used as chelators.

Received: November 11, 2014
Accepted: January 26, 2015

DOI: 10.1021/ac504213q
Anal. Chem. XXXX, XXX, XXX−XXX

Scheme 1. Schematic Illustration of Ion-Selective Nanospheres as Optical Indicator and Chelator for Complexometric Titration

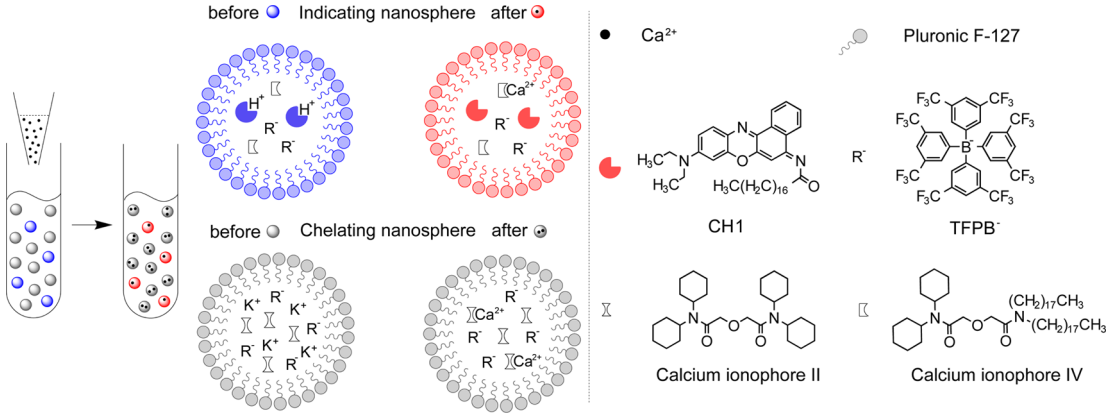

EXPERIMENTAL SECTION

Reagents. Pluronic F-127 (F127), *o*-nitrophenyl octyl ether (*o*-NPOE), dodecyl *o*-nitrophenyl ether (*o*-NPDDE), tetrahydrofuran (THF), sodium tetrakis-[3,5-bis(trifluoromethyl)-phenyl]borate (NaTFPB), potassium tetrakis[3,5-bis-(trifluoromethyl)phenyl]borate (KTFPB), calcium ionophore II (ETH 129), chromoionophore I (CH1), calcium ionophore IV, poly(vinyl chloride) (PVC), sodium hydrogen carbonate ($NaHCO_3$), hydrochloric acid (HCl), nitric acid (HNO_3, super pure), and calcium chloride ($CaCl_2$) were obtained from Sigma-Aldrich. Standard reference material (1643e, trace elements in water) was obtained from the National Institute of Standard and Technology (NIST).

Preparation of Chelating and Indicating Nanospheres. To prepare the chelating nanospheres, typically 2.27 mg of ETH129, 1.24 mg of KTFPB, 8.0 mg of *o*-NPDDE, and 3.0 mg of F127 were dissolved in 2.0 mL of THF to form a homogeneous solution. The THF solution (0.5 mL) was pipetted and injected into 3 mL of deionized water on a vortex with a vortexing speed of 1000 rpm. Compressed air was blown on the surface of the resulting nanosphere emulsion for 30 min to remove THF. To prepare the indicating nanospheres, typically 5.66 mg of calcium ionophore IV, 0.75 mg of CH1, 1.78 mg of NaTFPB, 8.0 mg of *o*-NPOE, and 5.0 mg of F127 were dissolved in 3.0 mL of THF to form a homogeneous solution. The same procedure as mentioned above was used to fabricate the nanospheres.

Instrumentation. Optical titration signals were measured with a UV−visible absorption spectrometer (SPECORD 250 plus, Analytic Jena, AG, Germany).

Optical Titration. For this procedure, 2.5 or 3 mL of the chelating nanospheres (complexing agent) and 20 μL of the indicating nanospheres (indicator) were mixed in a cuvette. The optical reverse titrations were performed by stepwise aliquoting 10^{-3} M $CaCl_2$ or the standardized sample into the titration cuvette, each followed with recording of absorption spectrum.

RESULTS AND DISCUSSION

Scheme 1 shows the principle of the reverse titration of calcium. A small amount of indicating nanospheres was mixed with excess amount of chelating nanospheres. The titrant (Ca^{2+} containing aqueous samples) was then dosed to the nanosphere emulsion. The indicating nanospheres contained calcium ionophore IV, CH1, NaTFPB, embedded in the hydrophobic nanosphere core made of *o*-NPOE and F127. The chelating nanospheres had similar sensing components (KTFPB, ETH 129, and *o*-NPDDE)[9] but lacked the chromoionophore. Different ionophores and matrices were used here to help ensure that the chelating particles exhibit a higher calcium affinity than the indicating particles. The different matrices may also reduce the exchange of components between the two types of particles.

Compared with conventional titrations, both the complexation reaction and the end point indication have been moved from the aqueous phase to an organic phase. With more titrant (Ca^{2+}) added, the chelating particles will eventually become saturated, resulting in an increase of the free calcium concentration in solution. At that point, calcium will be extracted into the indicating particles and causes the deprotonation of CH1, which then results in a change in absorbance and color. The amount of Ca^{2+} added can be quantified by the total amount of ion-exchanger (TFPB) if ionophore is in sufficient excess.

The nanospheres are fabricated by a precipitation method,[22] where the hydrophobic sensing components self-assemble into the nanosphere core. The typical average diameter of the nanospheres is less than 100 nm, but may grow with increasing particle concentration.[9,22] The indicating nanospheres have been reported as exhaustive nanosensors that are extremely sensitive to the analyte.[20,21] For instance, with small nanosphere quantities, 10^{-7} M of Ca^{2+} is able to cause complete deprotonation of CH1, thereby changing the color of the nanosphere emulsion from blue to red.

For the calcium-selective chelating nanospheres, the working mechanism can be understood with the extraction process between the aqueous (aq) and organic nanospheric (ns) phase as shown in eq 1.

$$Ca^{2+}(aq) + 2M^{+}(ns) + 3L(ns) \rightleftharpoons CaL_3^{2+}(ns) + 2M^{+}(aq) \quad (1)$$

where M^+ is the initial counterion of the ion exchanger in the nanosphere, L is the calcium ionophore that forms complexes of the type CaL_3^{2+}.

For the indicating nanospheres that contain an additional chromoionophore (*Ind*), a similar extraction process is shown in eq 2, where $HInd^+$ is the protonated chromoionophore.

$$Ca^{2+}(aq) + 2HInd^{+}(ns) + 3L(ns) \rightleftharpoons CaL_3^{2+}(ns) + 2H^{+}(aq) + 2Ind(ns) \quad (2)$$

The indicating nanospheres are subjected to an additional competition between hydrogen ions and calcium. By lowering the sample pH and/or the acidity of the chromoionophore, the calcium uptake capability should be weakened to a significant extent. Therefore, the difference in calcium affinity between the

DOI: 10.1021/ac504213q
Anal. Chem. XXXX, XXX, XXX−XXX

two varieties of nanospheres makes them promising candidates as indicators and complexants in complexometric titrations.

The relationship between primary ion (Ca^{2+}) concentration in the sensing phase and the sample solution can be quantified on the basis of ion-exchange theory. Both the indicating and the chelating nanospheres contain an excess of ionophore relative to ion exchanger. The mole fraction of Ca^{2+} (in the complex form) in the chelating nanospheres and the indicating nanospheres can be described by eqs 3 and 4, respectively, where $[CaL_3^{2+}]^{cs}$ and $[R^-]^{cs}$ are the concentrations of Ca^{2+} and TFPB in the chelating nanospheres, respectively. $[Ca^{2+}]^{aq}$,$[J^+]^{aq}$ and $[J^{+\prime}]^{aq}$ are the concentration of Ca^{2+} and interfering ions in the sample solution, respectively. $K^{cs}_{Ca^{2+},J^+}$ is the selectivity coefficient for the chelating nanosphere while $[CaL_3^{2+}]^{is}$, $[R^-]^{is}$ and $K^{is}_{Ca^{2+\prime},J^{+\prime}}$ are the corresponding values for the indicating nanospheres.

$$\frac{2[CaL_3^{2+}]^{cs}}{[R^-]^{cs}} = \frac{2[Ca^{2+}]^{aq} + (K^{cs}_{Ca^{2+},J^+}[J^+]^{aq})^2}{2[Ca^{2+}]^{aq}} - \frac{\sqrt{4[Ca^{2+}]^{aq}(K^{cs}_{Ca^{2+},J^+}[J^+]^{aq})^2 + (K^{cs}_{Ca^{2+},J^+}[J^+]^{aq})^4}}{2[Ca^{2+}]^{aq}} \quad (3)$$

$$\frac{2[CaL_3^{2+}]^{is}}{[R^-]^{is}} = \frac{2[Ca^{2+}]^{aq} + (K^{is}_{Ca^{2+\prime},J^{+\prime}}[J^{+\prime}]^{aq})^2}{2[Ca^{2+}]^{aq}} - \frac{\sqrt{4[Ca^{2+}]^{aq}(K^{is}_{Ca^{2+\prime},J^{+\prime}}[J^{+\prime}]^{aq})^2 + (K^{is}_{Ca^{2+\prime},J^{+\prime}}[J^{+\prime}]^{aq})^4}}{2[Ca^{2+}]^{aq}} \quad (4)$$

The total amount of Ca^{2+} can be divided into three fractions, those in the chelating nanospheres, in the indicating nanospheres, and in the sample solution, as shown in eq 5.

$$[Ca^{2+}]^{titrant} V^{titrant}_{Ca^{2+}} = [CaL_3^{2+}]^{cs} V^{cs} + [CaL_3^{2+}]^{is} V^{is} + [Ca^{2+}]^{aq} V_T \quad (5)$$

where $[Ca^{2+}]^{titrant}$ is the concentration of Ca^{2+} in the titrant, $V^{titrant}_{Ca^{2+}}$ is the volume of the titrant, V^{cs}, V^{is} are the volumes of the chelating nanospheres and the indicating nanospheres, respectively, V_T is the total volume.

Base on charge balance, the relationship between the protonated *CH1* ($HInd^+$) in the indicating nanospheres and ion exchanger TFPB is shown in eq 6.

$$[HInd^+]^{is} = [R^-]^{is} - 2[CaL_3^{2+}]^{is} \quad (6)$$

where $[HInd^+]^{is}$ is the concentration of the protonated *CH1* in the indicating nanospheres.

The optical signal, absorbance (A), in this case, is expressed in eq 7.

$$A = \varepsilon_{HInd^+} b[HInd^+]^{is} + \varepsilon_{Ind} b([Ind_T]^{is} - [HInd^+]^{is}) \quad (7)$$

where $[Ind_T]^{is}$ is the total concentration of *CH1*, ε_{HInd^+} and ε_{Ind} are the molar extinction coefficients, and b is the optical path length.

Equation 8 is obtained after inserting eq 6 to eq 7:

$$A = \varepsilon_{Ind} b([Ind_T]^{is} - [R^-]^{is} + 2[CaL_3^{2+}]^{is}) + \varepsilon_{HInd^+} b([R^-]^{is} - 2[CaL_3^{2+}]^{is}) \quad (8)$$

Finally, $V^{titrant}_{Ca^{2+}}$ as a function of A can be obtained by solving eqs 3, 4, 5, and 8 (see eq S1 in Supporting Information).

The optical reverse titration for Ca^{2+} at different pH can now be predicted, as shown in Figure 1. The vertical dashed line indicates the expected end point. At acidic pHs, sigmoidal titration curves are expected. With increasing pH, the s-shape curves change to two linear lines. Note that at very low pH (pH 1.5), the titration curve is flat because CH1 cannot be deprotonated even in the presence of excess amount of Ca^{2+}. At pH 7.5, the end point can be determined at the intersection of two lines. Figure S1 and S2 show the simulation of the concentration of Ca^{2+} in the chelating nanospheres, the indicating nanospheres and aqueous phase during the addition of titrant at pH 7.5 and pH 5.5, respectively. A linear relationship between Ca^{2+} exchanged into the indicating nanospheres and the volume of titrant was obtained, meaning that the indicating nanospheres are working in the exhaustive mode at pH 7.5 (Figure S1b). Therefore, a linear relationship between the absorbance A and $2n_{Ca^{2+}}$:n_{TFPB} (Figure 1) was obtained. This lack of s-shaped curve is understood by a proportionality between calcium content in the two types of particles, whereas the calcium level in the aqueous solution remains insignificant before the end point. At pH 5.5, the Ca^{2+} exchanged into the indicating nanospheres as a function of volume of titrant assumes an s-shaped curve (Figure S2b) which signifies a sigmoidal relationship between A and $2n_{Ca^{2+}}$:n_{TFPB} (Figure 1).

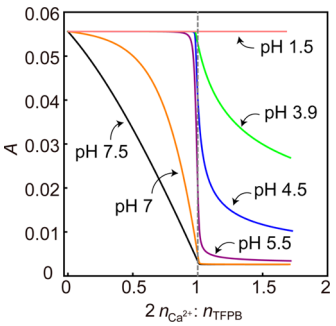

Figure 1. Theoretical optical reverse titration curves for calcium in different pH conditions. *A* is the absorbance at protonated wavelength. The dashed vertical line indicates the expected end point.

Figure 2 shows the theoretical titration curves simulated with different amounts of indicating nanospheres (different C_{is}) at pH 7.5. The titration end point gradually moves further away from the expected end point with increasing amount of indicating nanospheres. This is because the indicating nanospheres will consume analytes themselves. In this situation, not only the concentration of ion exchanger in the chelating nanospheres but also that in the indicating nanospheres should be accounted for.

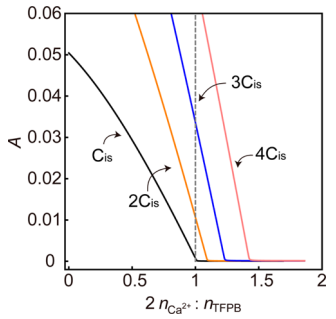

Figure 2. Theoretical reverse titration curves for calcium at pH 7.5 by using different amount of indicating nanospheres. C_{is} represents a fixed concentration of indicating nanospheres. *A* is the absorbance at protonated wavelength. The dashed vertical line indicates the expected end point.

DOI: 10.1021/ac504213q
Anal. Chem. XXXX, XXX, XXX−XXX

Figure 3 shows the experimental optical reverse titration curve (a) and absorption spectra (b) for Ca^{2+}. The titration was

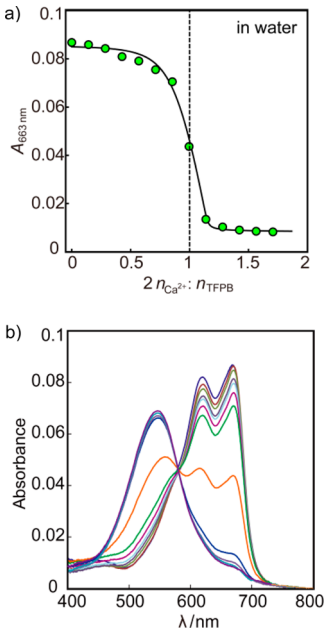

Figure 3. (a) Reverse titration curve for calcium titration using 10^{-3} M $CaCl_2$. End point indicator: exhaustive Ca^{2+}-selective nanospheres. Chelator: nanospheres containing ETH 129 and TFPB. (b) Absorption spectra recorded at each titration point.

performed in nonbuffered water. A 10^{-3} M $CaCl_2$ solution (titrant) was gradually added to the mixed nanosphere emulsion. Before addition of any Ca^{2+}, the emulsion exhibited a blue color owing to the complete protonation of CH1. As more Ca^{2+} was added, the protonation peak gradually decreased because of a small increase in the free Ca^{2+} level. At first, the decrease was quite small and gradual because most of the titrant was consumed by the chelating nanospheres. After saturation of the indicating nanospheres, the free Ca^{2+} concentration increase could be detected by the indicating nanospheres, giving a sharp transition with a very small error (ca. 1%). Indeed, the end point was obtained at 70 μL ± 0.5 μL (standard deviation), whereas the expected value was at 70.3 μL. The result corresponds satisfactorily to the expected theoretical s-shaped curve. Note that the sharpness of the transition highly depends on the interaction between the indicator and the analyte, which is defined by the optode response function as explained below.

Conventional titration using organic chelators and indicators usually requires pH control because any pH change could influence the effective binding strength of the chelator or the indicator molecule. The chelating nanospheres do not suffer from this disadvantage because the calcium ionophores are not pH-sensitive in a wide pH range. In addition, the exhaustive indicating nanospheres have been known to be pH-independent within a defined window of pH.[20] Figure 4 shows that the Ca^{2+} titration in different pH conditions. Even at very low pH value (pH 2.9, HNO_3), an accurate end point can still be obtained. Admittedly, under these acidic conditions, the absorbance change is much smaller than at more elevated pH because CH1 cannot undergo complete deprotonation. Indeed, chromoionophores with different basicities are available, providing the opportunity for a tunability of the working pH window and sensitivity of the indicating particles. Note that there

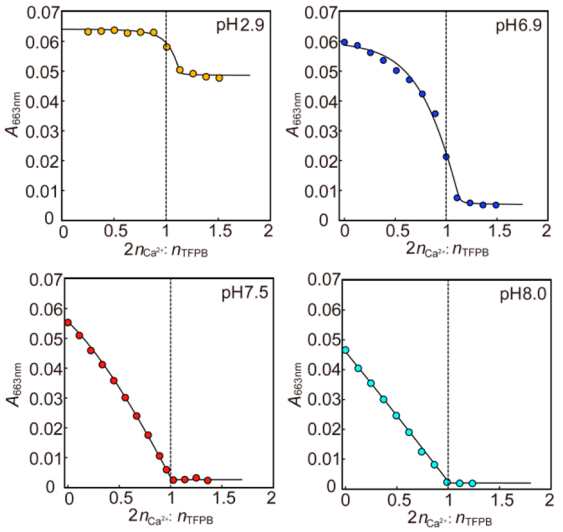

Figure 4. Experimental optical reverse titration curves for calcium in different pH solution. The dashed vertical lines indicate the expected end point. The pH 2.9 solution was prepared diluting HNO_3. The pH 6.9, pH 7.5, and pH 8.0 buffer solutions were prepared adjusting 10^{-3} M $NaHCO_3$ with HCl solution.

exist no traditional calcium chelators and optical indicators that allow one to titrate calcium at this pH.

CH1 deprotonates more readily if the optical titration is performed at higher pH (Figure 4). The end point was at the transition point of the s-shaped titration curve, which gradually became more linear with increasing pH (as discussed above). At pH 7.5 and pH 8.0, the end point is found at the intersection of two linear curves (compare to Figure 1). The titration curves correspond indeed well to theoretical expectations, and the errors are very small (ca. 1%). Further work will aim to improve the sharpness of the observed end point further to match those with potentiometric detection.[9]

The consumption of analyte by the indicating nanospheres can be neglected if the amount of the indicating nanospheres is sufficiently small. However, if a high amount of indicating nanospheres was used, the ion exchanger in the indicating nanospheres cannot be ignored. Figure 5 shows the optical reverse titration for calcium with a large amount of indicating nanospheres. When the total amount of ion exchanger in both

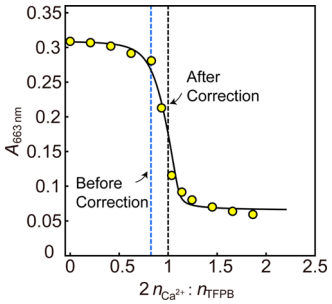

Figure 5. Optical reverse titration curve for calcium in nonbuffered sample solution containing larger amount of indicating nanospheres. C_{TFPB} (chelating nanospheres) = 5.2×10^{-5} M, C_{TFPB} (indicating nanospheres) = 1.2×10^{-5} M, V_{total} = 3 mL. A 10^{-3} M $CaCl_2$ stocking solution was used as titrant. Black and blue dashed vertical lines indicate the expected end point with and without considering the TFPB in the indicating nanospheres.

DOI: 10.1021/ac504213q
Anal. Chem. XXXX, XXX, XXX−XXX

the chelating and the indicating nanospheres is accounted for, the error was very small (ca. 1.1%). If only those in the chelating particles were taken into account, the error was 17.9%.

In order to know if the sensing components in chelating and indicating nanospheres will exchange with each other, the change of absorbance of a mixture of two types of nanospheres was observed over time in 10 mM tris-HCl buffer at pH 7. One type of nanosphere contained only CH1 and the other just NaTFPB, whereas the matrix of the nanospheres were the same. If the components exchange, some nanospheres containing both CH1 and NaTFPB will appear. At such experimental conditions, CH1 will become fully protonated in the mixed nanospheres, while it remains fully deprotonated in the nanospheres containing CH1 only since no ion exchanger exists. As shown in Figure 6, the

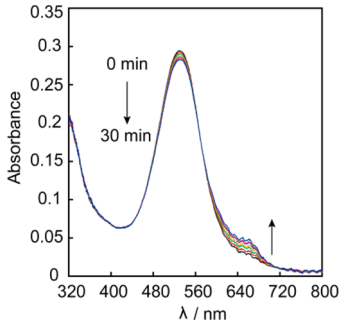

Figure 6. Time response of two types of nanospheres mixed in 10 mM tris-HCl buffer solution at pH 7. One contains only CH1 and the other only NaTFPB. The final concentration for CH1 and NaTFPB is 1.27×10^{-5} M and 1.58×10^{-5} M, respectively.

absorbance peak at 531 nm (deprotonation peak) and 663 nm (protonation peak) only showed a small change during 30 min. Note that one titration process takes less than 5 min. This confirms that the interchange of the components in the chelating and the indicating nanospheres is negligible.

The calcium level in a standardized reference sample (synthetic sample with standardized ion concentration) was determined. As shown in Figure 7, the result from the optical titration was found to be in agreement with the value of the standardized sample. This also suggests that the selectivity of the calcium-selective nanospheres is sufficient for routine analysis of fresh water.

In conclusion, we proposed here for the first time the use of ion-selective nanospheres as optical indicator as well as

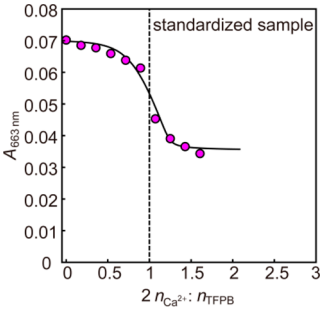

Figure 7. Reverse titration of Ca^{2+}-selective nanospheres using standard reference material 1643e as titrant. The dashed vertical line indicates the expected end point. C_{TFPB} (chelating nanospheres) = 3.61×10^{-5} M, V_{total} = 2.5 mL. The standardized concentration of calcium in reference material 1643e is 8.06×10^{-4} M.

complexing agents for complexometric titrations. The titrations can be performed in a wide range of pH, which is impossible to achieve with existing calcium chelators. The nanospheres showed excellent selectivity and sensitivity for calcium. The calcium level in standardized sample was successfully assessed.

■ ASSOCIATED CONTENT

Ⓢ Supporting Information

Additional information as noted in the text. This material is available free of charge via the Internet at http://pubs.acs.org.

■ AUTHOR INFORMATION

Corresponding Author

*E-mail: eric.bakker@unige.ch.

Notes

The authors declare no competing financial interest.

■ ACKNOWLEDGMENTS

The authors thank the Swiss National Science Foundation (SNF) and the University of Geneva for financial support. Jingying Zhai gratefully acknowledges the support by the China Scholarship Council.

■ REFERENCES

(1) Schwarzenbach, G.; Flaschka, H. *Complexometric titrations*; Methuen: London, 1969.
(2) Christian, G. D. *Analytical Chemistry*; John Wiley & Sons, Inc.: New York, 2004.
(3) Scott, L. E.; Orvig, C. *Chem. Rev.* **2009**, *109*, 4885.
(4) Buccella, D.; Horowitz, J. A.; Lippard, S. J. *J. Am. Chem. Soc.* **2011**, *133*, 4101.
(5) Pandey, U.; Dhami, P. S.; Jagesia, P.; Venkatesh, M.; Pillai, M. R. A. *Anal. Chem.* **2008**, *80*, 801.
(6) Peper, S.; Ceresa, A.; Bakker, E.; Pretsch, E. *Anal. Chem.* **2001**, *73*, 3768.
(7) Yin, P.; Li, T.; Forgan, R. S.; Lydon, C.; Zuo, X.; Zheng, Z. N.; Lee, B.; Long, D.; Cronin, L.; Liu, T. *J. Am. Chem. Soc.* **2013**, *135*, 13425.
(8) Reilley, C. N.; Schmid, R. W.; Sadek, F. S. *J. Chem. Educ.* **1959**, *36*, 555.
(9) Zhai, J.; Xie, X.; Bakker, E. *Chem. Commun.* **2014**, *50*, 12659.
(10) Reilley, C. N.; Schmid, R. W. *Anal. Chem.* **1958**, *30*, 947.
(11) Duso, A. B.; Chen, D. D. Y. *Anal. Chem.* **2002**, *74*, 2938.
(12) Krüger, R.; Pfenninger, A.; Fournier, I.; Glückmann, M.; Karas, M. *Anal. Chem.* **2001**, *73*, 5812.
(13) Trimukhe, K. D.; Varma, A. J. *Carbohydr. Polym.* **2008**, *71*, 66.
(14) Harvey, A. E.; Komarmy, J. M.; Wyatt, G. M. *Anal. Chem.* **1953**, *25*, 498.
(15) Männel-Croisé, C.; Meister, C.; Zelder, F. *Inorg. Chem.* **2010**, *49*, 10220.
(16) Afshar, M. G.; Crespo, G. A. *Anal. Chem.* **2012**, *84*, 8813.
(17) Bakker, E.; Bühlmann, P.; Pretsch, E. *Chem. Rev.* **1997**, *97*, 3083.
(18) Xie, X.; Mistlberger, G.; Bakker, E. *J. Am. Chem. Soc.* **2012**, *134*, 16929.
(19) Xie, X.; Bakker, E. *ACS Appl. Mater. Interfaces* **2014**, *6*, 2666.
(20) Xie, X.; Zhai, J.; Bakker, E. *Anal. Chem.* **2014**, *86*, 2853.
(21) Xie, X.; Zhai, J.; Crespo, G. A.; Bakker, E. *Anal. Chem.* **2014**, *86*, 8770.
(22) Xie, X.; Mistlberger, G.; Bakker, E. *Anal. Chem.* **2013**, *85*, 9932.

DOI: 10.1021/ac504213q
Anal. Chem. XXXX, XXX, XXX−XXX